SPACE VEHICLE PROPULSION SYSTEMS:

ENVIRONMENTAL SPACE HAZARDS

NASA Grant No. NAG 3-948

Final Report

Prepared for: National Aeronautics and Space Administration
Lewis Research Center, MS 500-315
21000 Brookpark Road
Space Propulsion Technology Division
Cleveland, Ohio 44135

Submitted by: Dr. P.J. Disimile
Dr. G.K. Bahr

NASA Center for Health Monitoring of Space Propulsion Systems and the
Department of Aerospace Engineering and Engineering Mechanics

September, 1990

ABSTRACT

The purpose of this research is to evaluate the hazards that exist in geo-lunar space which may degrade, disrupt or terminate the performance of space-based LOX/LH2 rocket engines. Accordingly, this report provides a summary of the open literature pertaining to geo-lunar space hazards.

Approximately 350 citations and about two hundred documents and abstracts were reviewed; the documents selected give current and quantative detail. The methodology was to catagorize the various space hazards in relation to their importance in specified regions of geo-lunar space. Additionally, the effect of the various space hazards in relation to spacecraft and their systems were investigated.

It was found that further intensive investigation of the literature would be required to assess the effects of these hazards on propulsion systems per se; in particular, possible degrading effects on exterior nozzle structure, directional gimbals, and internal combustion chamber integrity and geometry.

Acknowledgements:

The work described herein was supported by NASA under Grant No. 3-948. The authors would like to thank Dr. S.G. Rubin of the NASA Center, University of Cincinnati, and Messrs. Marc Millis and Mike Binder of the Lewis Research Center for their patience and support.

TABLE OF CONTENTS

LIST OF FIGURES

LIST OF TABLES

1.0 INTRODUCTION

The purpose of this research is the evaluation of the hazards that exist in geo-lunar space which have the potential to degrade, disrupt or terminate the performance of LOX/LH2 rocket engines. The objective of this investigation is to examine, study and assess the open literature pertaining to these hazards.

The plan of investigation was that of a selective literature search; candidate documents are selected that give current and quantative detail. Also included are those articles and treatises of classic and modern vintage that are written in the context of detailed review. Thus far the methodology has been to study space hazards in order of their prevasiveness, then examine them, in relation to their importance in a specified region of geo-lunar space.

Results and conclusions come from various documents both general and specialized that address space hazards in relation to spacecraft and all their systems in the geo-lunar domain. From approximately 350 citations about two hundred documents and abstracts have been reviewed; obviously this meager number does not begin to represent the wealth of applicable and potentially useful literature available on this subject.

1.1 An Overview of Space Hazards and Locales

We now consider various space hazards with respect to their locale. In order to give the reader a "bird's eye view" of the overall picture, we shall list the various space hazards of interest, coupled with the regions of geo-lunar space where they apply. First, the various space hazards and space locales are specified in detail, along with graphic presentation of their interactions.

Broadly speaking, pertinent space hazards fall into four categories; (1) radiation, (2) meteoroids, (3) monatomic oxygen and, (4) thermal gradients and shock. They are listed in detail in Table I.

Table I. SPACE HAZARDS

Space Hazards and Description	Comments
a. Cosmic initiated gamma rays	(extremely hard ionizing electromagnetic radiation)
b. Charged particle plasma (solar wind)	[ionizing x-rays, also non-ionizing radiation (U.V.), electrons (e^-), protons (^+H), and neutrons ($^\circ n$)].
c. Meteoroids, cometary and astroidal	ranging from dust (mean particulate mass 10^{-6} grams), up to particulate mass of $\simeq$ 1 gram.
d. Monatomic oxygen degradation	
e. Thermal gradients and shock	

On consulting Table I, it is to be noted that radiation is considered in the context of two modalaties, in that it is fundamentally of a wave (photon) nature, and of a particulate nature, as indicated in (a) & (b).

Inasmuch as the earth-moon system is of primary interest for upcoming missions, one now considers the detailed specification of this environment as shown in Table II on the following page.

Table II. GEO-LUNAR SPACE

	Geo-Lunar Region, Defined
(a-s)	Low Earth Orbit (L.E.O.) circular ≃ 300-500 km
(b-s)	Geo-Synchronous Orbit (G.E.O.) ≃ 35,800 km at ≃ twenty-three degrees W.R.T. the ecliptic.
(c-s)	L.E.O. - G.E.O. transfer trajectories
(d-s)	Low Lunar Orbit (L.L.O.) ≃ 100 km altitude
(e-s)	L.L.O. Transfer Trajectories (lunar surface) (L.L.O. L.S.)
(f-s)	Lunar Surface (L.S.)

Now that one has the space hazards and environment defined we shall consider possible interactions between said hazards and various space locales.

When one considers interaction between a given space locale and hazard, there are, as indicated in Table II but four null interactions out of a possible thirty; accordingly we now embark on a detailed discussion of the various space hazards themselves.

TABLE III. SPACE HAZARD VS. LOCALE

	Space Hazard				
Space Locale	(a)	(b)	(c)	(d)	(e)
(a-s)	x	x	x	xx	xx
(b-s)	xx	xx	x	--	xx
(c-s)	xx	x	x	x	x
(d-s)	xx	x	xx	--	xx
(e-s)	xx	x	xx	--	x
(f-s)	xx	x	xx	--	x

xx strong interaction present x interaction present - little if any interaction

With the arena of interest specified in detail in Tables I,II along with specific interactions shown in Table III we now embark on a detailed study of the hazards themselves in relation to our specified environment.

2.0 SPACE HAZARDS

2.1 Radiation

In discussing the various aspects of radiation hazard, one must appreciate that we are dealing with several types of radiation, which fall into the pedestrian categories of waves and particles, all of which are present in relative abundances given below. It is essential to understand that both ionizing and non-ionizing radiation produce deleterious effects peculiar to themselves. In addressing the bifurcation of ionizing vs. non-ionizing radiation, there is a distinct region of overlap in the geo-lunar environment. For our purposes the "cut-off" for ionizing radiation may be taken to be the first ionizing potential of hydrogen. Unavoidably, the demarkation for charged and neutral particle radiation (Bremsstrahlung) is much less easily defined. This situation comes about because possible ionizing electromagnetic radiation is by virtue of the local acceleration of charged particles rather than from direct primary and secondary sources ("cosmic radiation", i.e. high energy neutrons and protons of galactic and extra-galactic origin, together with protons, electrons and neutrons of solar origin). Quantitating this class of hazards in the geo-lunar domain is fraught with uncertanties, the primary one being the inability to forecast solar flares over a short time period as opposed to the ten year period observed by H. Schwabe, Ref. 5, p. 25. More recently this time interval has been extended to approximately eleven years with an event frequency spread about an activity peak ranging from seven to thirteen

years. One could assert that predicting levels of ionizing radiation from solar flares is analogous to forecasting weather here on earth.

We will now consider some important parameters that specify solar high energy particulate radiation; to deal with such a problem one must develop a probabilistic model for solar flare disturbances, based on long term observations. The model presented here applies in our spatial locale of interest, the region intervening the earth-moon system as well as surrounding it.

The following is purported to be a quantitative description of approximate cosmic abundances of particulate radiation constituents: from all possible sources in the universe: (geolunar environment)

a. $\simeq$ 85% protons (H^+)

b. $\simeq$ 14% alpha particles (He^{++})

c. $\simeq$ 1% nuclii of elements from Li^+ to Fe^+ on the Periodic Table

In reference to this aspect of the geo-lunar environment the source document[1] does not explicitly state the methods of making the above determinations, but gives ample references to them. In any event the following synopsis of the "earth observed" data is now presented in Table IV.

TABLE IV. SOLAR HIGH ENERGY, PARTICULATE PARAMETERS

flux sunspot maximum	1.5 (particles/cm^2)/sec (isotropic)
integrated yearly rates	5×10^7 particles/cm^2
energy range	100 Mev to 10^{19} Mev preponderance of energy 10^9 to 10^{13} ev
integrated dosage	6 to 20 rads/yr. or 0.6 to 2.2 millirads/hr.
flux at sunspot minimum	4 (particles/cm^2)/sec (isotropic)
integrated yearly rates	1.2×10^8 particles/cm^2
solar high energy particle radiation (Ref. (1) p. 4 & 5)	In the following tabulations N_α = the number of protons/sec and N_p is given by the number of alpha particles/sec.
Integrated Yearly Flux	Solar maximum energy > 30 Mev, 3.5×10^9 particles/cm^2

In the following tabulations N_p = the Solar maximum energy > 100 Mev, the number of protons/sec and N_R = the 3.5×10^8 particles/cm^2 the number of alpha particles/sec.

75 rem/yr. at solar maximum with 5 gram/cm^2 shielding

1 rem/yr. at solar minimum

Note that it is well understood that the ratio $\frac{N_p H^+}{N_\alpha H_e^{++}}$ depends upon solar activity; however, it is customary in the case of preliminary calculations to take this ratio as unity, also due to low abundances the nuclii listed in item c) above are ignored.

It should be observed that for the solar minimum, one has the same spectral distribution for the integrated flux in Table V; however, the total particle flux is reduced to 10^6 particles/cm^2. The associated average ionizing dose rates are, with 5 gram/cm^2 shielding assumed (a typical

Table V. Probability of Choice - Solar Spectrum

Mission length, weeks	Probability, P			
	0.50	0.10	0.01	0.001
	N, protons/cm^2			
2	-	5.0×10^7	2.0×10^9	1.7×10^{10}
4	-	2.0×10^8	4.5×10^9	3.3×10^{10}
8	1.3×10^7	7.2×10^8	9.0×10^9	5.6×10^{10}
12	4.5×10^7	1.3×10^9	1.5×10^{10}	8.0×10^{10}
20	1.5×10^8	2.4×10^9	2.2×10^{10}	1.1×10^{11}
30	3.0×10^8	3.9×10^9	3.0×10^{10}	1.4×10^{11}
40	5.0×10^8	5.0×10^9	3.3×10^{10}	1.5×10^{11}
50	7.0×10^8	5.9×10^9	3.5×10^{10}	1.6×10^{11}
60	1.0×10^9	6.2×10^9	3.7×10^{10}	1.6×10^{11}
80	1.6×10^9	7.2×10^9	3.9×10^{10}	1.7×10^{11}
100	2.0×10^9	8.0×10^9	4.0×10^{10}	1.7×10^{11}

Typical time integrated spectral distributions :

$$N (> P) = N_0 \exp (- P / P_0)$$

spacecraft hull effective density) given at the bottom of Table IV where 1 rem = one rad equivalent man.

The above (Table IV) applies at one astronomical unit (A.U.) from the sun, and does not provide an accurate assessment for 0.5 A.U. to 1.75 A.U. which in our range of interest is not of importance for solar flares.

2.1.1 Solar Flares

Solar flare phenomena are particularly insideous, in that they, over short time intervals, arise by sheer chance. This puts their assessment into the realm of statistical vs. deterministic prediction. Considering the importance of modeling this phenomena, in virtue of all the deleterious particulate radiation associated with them, we shall spend some time on their proper assessment. The document[1] from which this data was taken gives a statistical model, the constants of which, would be the major variant, as more and more experimental data is accumulated, to give the model greater precision.

2.1.1a Mathematical Model for Solar Flare Hazard

The reference quoted now models this hazard by employing classical probability theory, considering the probability (p) of encountering more than N protons/cm^2 with rigidity (P) greater than 0.235 Bv for various mission durations. As an explanatory comment, the entities involved in electromagnetic and ionizing radiation do not obey the customary laws of Newtonian or classical mechanics, but rather the laws of relativistic electrodynamics and quantum mechanics. The so-called rigidity of a particle is simply its relativistic momentum divided by its charge, which from nuclear physics is the product of the magnitude of one unit of electronic

charge e^- and the stable state atomic number Z. The probability distribution of choice in constructing a solar spectrum is given in Table V. Although the spatial rate change of N_p, the number of (protons/sec)/cm^2 is unknown, the tabulated values may be used for 0.5 A.U. $\leq$ distance from sun $\leq$ 1.75 A.U. with an accuracy of one order of magnitude. Th concepts given here are from the discipline of relativistic field and particle physics; albeit, the method as applied here to solar flare radiation gives an excellent mathematical framework for modeling the phenomena in question.

First, one must give an explicit expression for the electromagnetic rigidity and other parameters necessary for formulating the expressions for specifying a model solar flare spectrum. In the reference document[1] the electromagnetic rigidity of a particle is designated by the symbol P, and takes the form

$$P = (\frac{1}{eZ})(T^2 + 2Tm_0c^2)^{1/2} \text{ ergs/esu}$$

where the variables are given by:

N = protons/cm^2 having a rigidity greater than P

P = rigidity in volts

P_0 = 97 Mev, a typical value for large events

N_0 = total event intensity, particles/m^2

eZ = nuclear charge (esu)

T = proton energy, (Mev)

m_0c^2 = proton rest energy; (ergs or Mev)

m_0c^2 = 938.2 Mev, for the proton

m_0c^2 = 3727.1 Mev, for the alpha particle

P_0 is evaluated for energies T $\geq$ 10 Mev, and the spectrum may be described by the expression $N\ (>T) \simeq N_0T^{-m}$ with m = 1.2. The typical model solar

flare spectrum assumes a form which gives the number of particles/cm^2 as a function of the total energy using the energy and rigidity as independent parameters:

$$T < 10 \text{ Mev} \quad : N(>T) = 72.8N(>239 \text{ Mv})T^{-1.2}$$

$$137 \text{ Mv} < P < 239 \text{ Mv} \quad : N(>P) = 35.5N(>239 \text{ Mv})e^{\frac{-P}{67}}$$

$$P \geq 239 \text{ Mv} \quad : N(>P) = 10.9N(>239\text{Mv})e^{\frac{-P}{100}}$$

It is evident that the "chance aspect" of the solar flare hazard is modeled here in a fashion consistent with the limits of human certitude. It would seem that an analogous modeling philosophy will prove valuable with other hazards as well.

2.1.2 Trapped Charged Particles

A second component to the overall radiation burden is the trapping of free electrons and protons by the earth's electromagnetic field in L.E.O., G.E.O. and L.L.O. If one studies the graphs in Figs. 1 and 2, it is evident that the limits of L.E.O., G.E.O. and L.L.O. bracket a region of maximum electron density, produced by, (in order of altitude from the earth) the overlapping of three broad layers of electron clouds, denoted as the E, F_1, and F_2 layers respectively. Detailed descriptions of these layers is beyond the scope of this report, and can be found in Reference (2). It should be noted that positively charged particles (protons) are also trapped by the earth's electromagnetic field with a different altitude distribution, and number flux distribution than electrons as shown for 400 km and 500 km altitudes, Loc. Cit. p. 42.

One can summarize "trapped charged particle" ionizing radiation in terms of its mechanism of production and its earth moon distribution.

2.1.2a Production Mechanism

Simply stated, the production of trapped charged particle ionization arises due to the interaction of the earth's magnetic field with solar emission (solar wind) and "cosmic rays".

2.1.2b Earth-Moon Distributions

The profiles of these various charged particle distributions are shown in Figs. 3, 4 and 5. The document's[2] distributions are understood to be modified by long as well as short term solar cycle variations; below G.E.O. fairly symmetric proton orbits exist, but variations day vs. night have been found to be of the order of a factor of four, while at lower altitude appear to be insensitive to local time effects at energies above 25 Mev. It turns out, however, that at approximately three earth radii, protons with a 1 Mev peak experience sizeable disturbances (variations).

2.1.3 Direct Cosmic Ray Effects

A third component to ionizing radiation insult is that of "cosmic radiation". This name was coined by R.A. Millikan, in that he established the existence (Circa 1930) of highly penetrating radiation based on his famous lakes arrowhead and muir experiments. Shortly after the discovery of radiation belts (Van-Allen May, 1958), it was suggested that cosmic neutrons

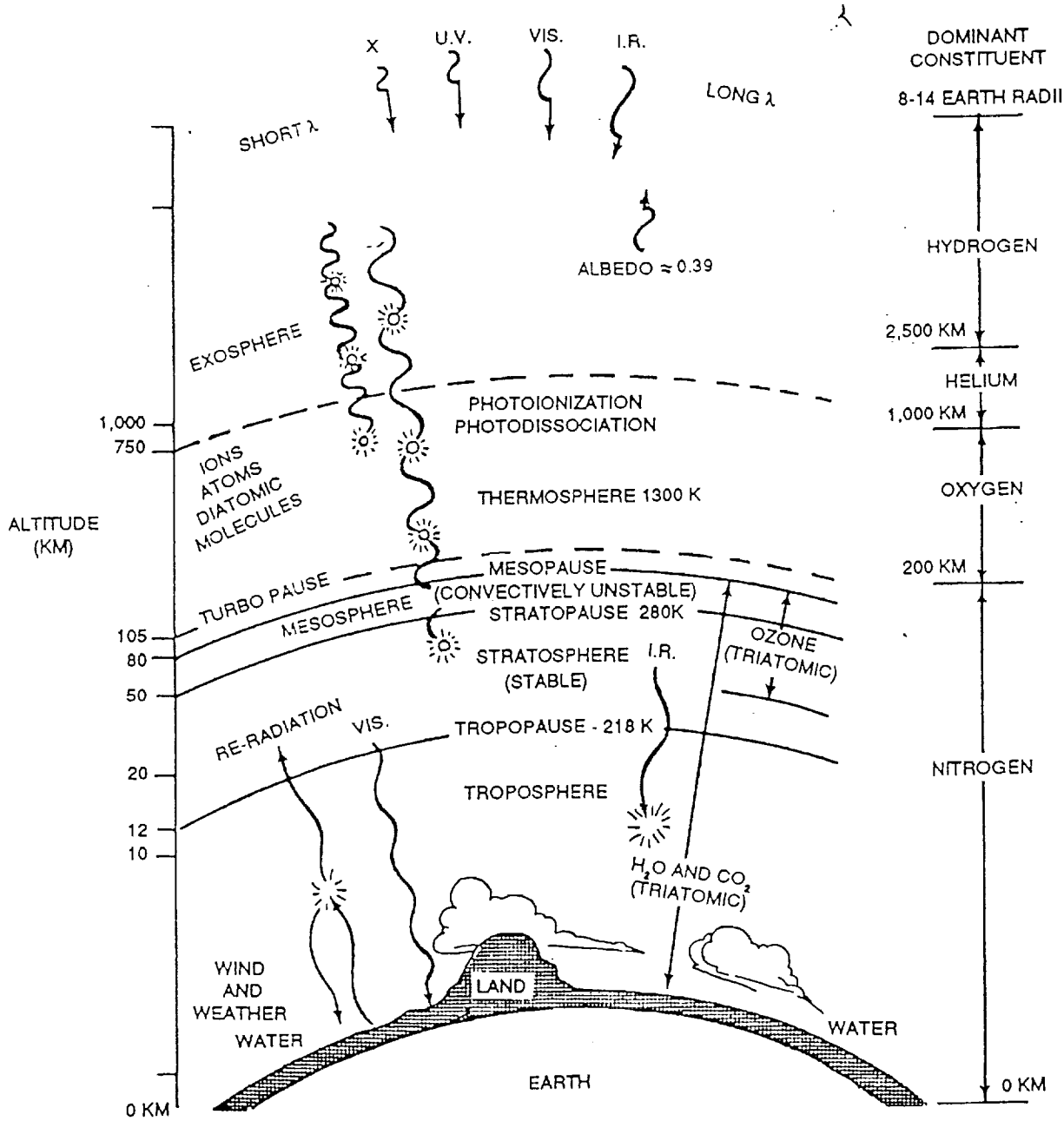

Fig. 1. Atmospheric chemical regimes *(after Carpenter et al., 1978).*

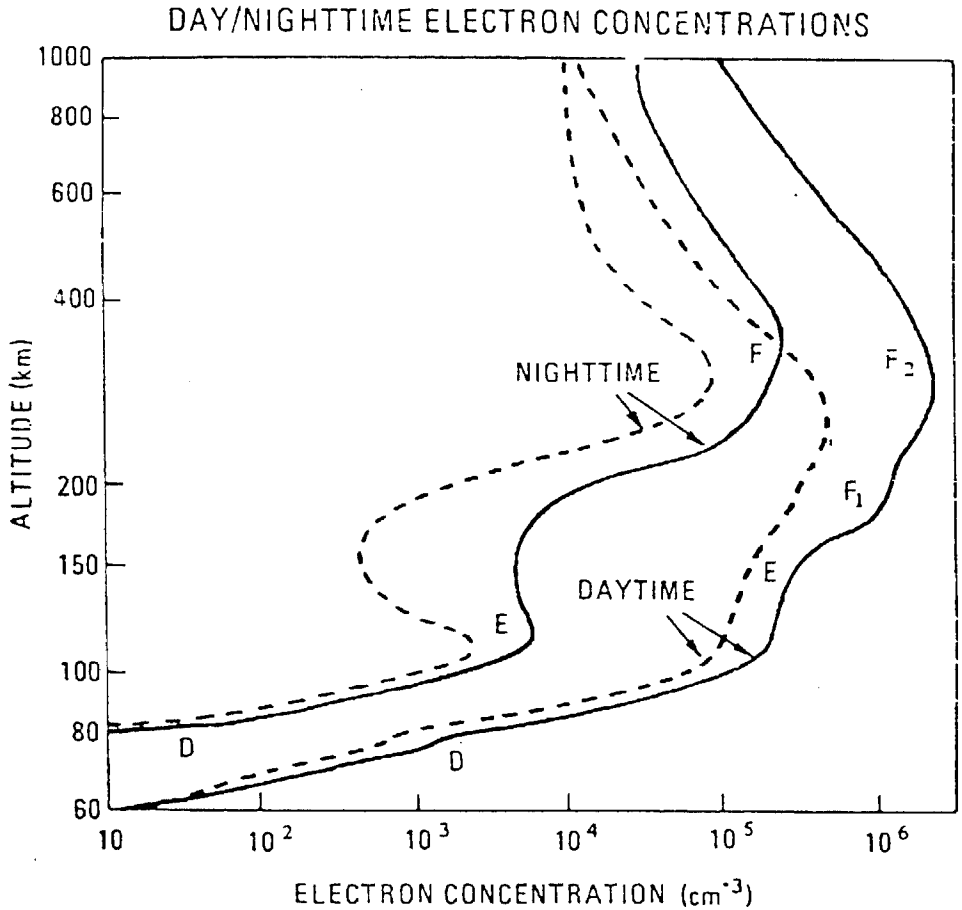

Fig. 2. Typical midlatitude daytime and nighttime electron density profiles for sunspot maximum (solid lines) and minimum (dashed lines).

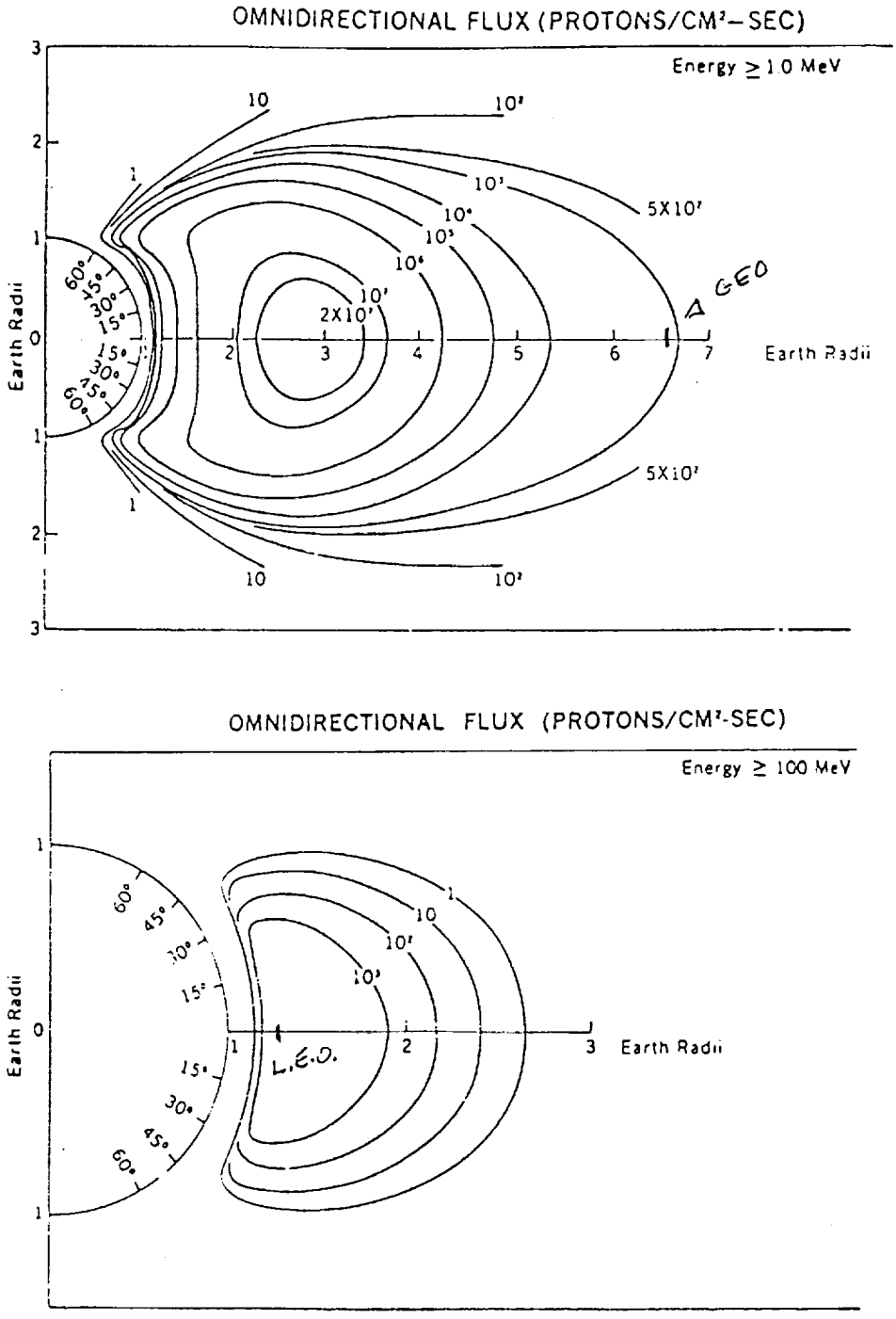

Fig. 3. A, Distribution of trapped protons with energy greater than 1 MeV. B, Distribution of trapped protons with energy greater than 100 MeV *(after Smith and West, 1983).*

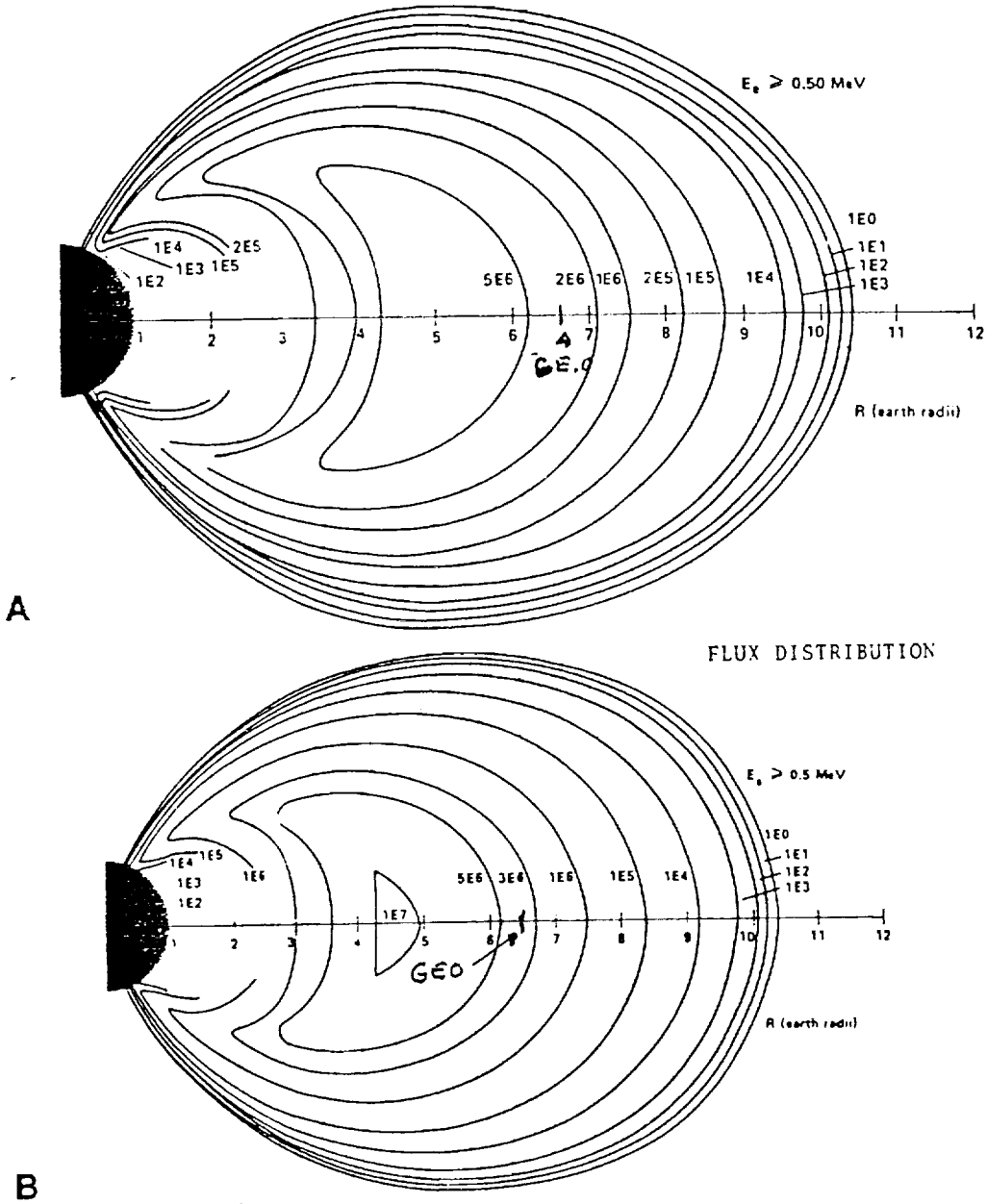

Fig. 4. (A) Distribution of trapped electrons during solar minimum with energy greater than 0.5 MeV. (B) Distribution of electrons with same energy during solar maximum. The notation "E" refers to the power of ten: 1E4 = 1×10^4 $cm^{-2}sec^{-1}$, etc. *(after Smith and West, 1983).*

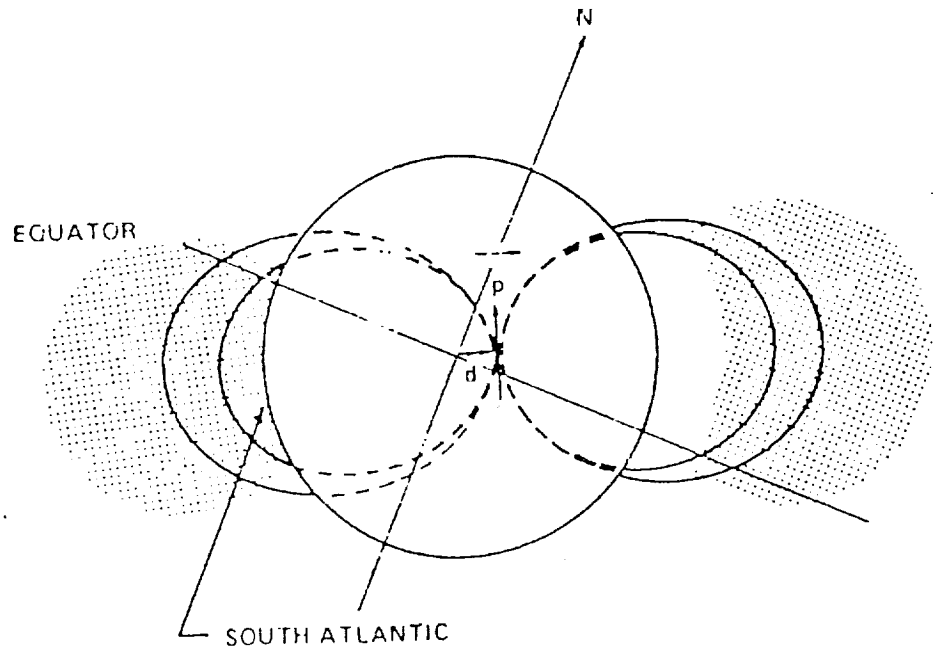

Fig. 5. Schematic showing that the radiation belts (shaded area) are lower in the South Atlantic anomaly due to the offset of the dipole field *(after West et al., 1977)*.

are the primary source; in this mechanism, primary "cosmic rays", protons of energy greater than 1 Gev, are incident on atomic nucelii composing the outer fringe of the atmosphere give rise to a sequence of nuclear events (reactions). A major product of these events is a neutron albedo flux (reflection flux). For this neutron albedo flux, the residency time in the upper atmosphere significantly exceeds the half life of a typical neutron (≃ 12 min.). Thus, neutron albedo decays into H^+, e^- pairs most of which becomes trapped by the earth's electromagnetic field, becoming part of the earth's "radiation belt". The above process is believed to be a source of protons whose energies exceed 50 Mev. Excluding radiation environmental safety for a crew on a protracted manned mission, the above described phenomena are, indeed, of great concern due to variation in "spacecraft drag profiles" and "spacecraft-system charging." The difficulty produced by unexpected changes in "spacecraft dragprofiles" is that of sending appropriate signals to the satellite for maintenance of desired orbital shape. Space-craft system charging can threaten the integrity of the satellite directly, thus it is proper to discuss this in relation to radiation hazard at this time.

2.1.3a Spacecraft-System Charging

Spacecraft-system charging has become a matter of much greater concern due to moden low voltage integrated circuit and chip technology now incorporated into space vehicle propulsion and navigational as well as communication control systems. This concern is far from the arena of supposition or hypothesis; this was borne out by an anecdotal experience with the pioneer spacecraft whose systems were almost terminated by the effects of trapped H^+ and e^- particles in the leviathan radiation belts of the planet Jupiter (Ref. 2, p. 97). Direct observation of this effect is

not confined to outer planetary excursions; it was clearly demonstrated by earth orbiting satellite ATS-6 which encountered and recorded surface potentials as high as 20,000 volts, said potential monitored with respect to the surrounding plasma through which it passed. Although it is true that the build-up of a large static charge with respect to the plasma environment can render necessary sensors useless for a time, (if not terminated); greater danger lies in abrupt differential discharge aided and abetted by differential external surface temperature (thermal) gradients (to be discussed in the sequel). The event of such discharge can produce a myriad of types of structural damage including functional parts of the propulsion system. Weak, abrupt differential discharges in L.E.O. or Jovian Planetary Orbit (J.P.O.) have been found to be responsible for the above host of malfunctions[2]. The malfunctions listed in (2), p. 97 are: (a) spurious electronic switching, (b) thermal breakdown of external vehicle coatings, (c) solar cell amplifier degradation and (d) reduction of efficiency of optical sensors. Note that (a) (c) and (d) can contribute indirectly to propulsion system malfunction, while (b) can have a direct effect. As far as the geo-lunar domain is concerned, a curious aspect of "space-craft system charging" is that it's most likely to occur in G.E.O.. The suggestion has been made that this may be peculiar to our mode of data acquisition in that a large number of high altitude satellites are in such an orbit. Consideration of the spatial distribution of the earth's magneto-sheath does suggest that orbits greater than four earth radii should, in principle, experience increased charging effects because of the position and orientation of solar-earth charged particle streaming; i.e. the earth literally has an ionization "tail" analogous to that of a comet. Approximate positioning of a typical geocentric orbit is shown in Figure 6.

To further escalate the charge-discharge problem are "cosmic rays." Particles in this extraordinary energy range can penetrate a spacecraft,

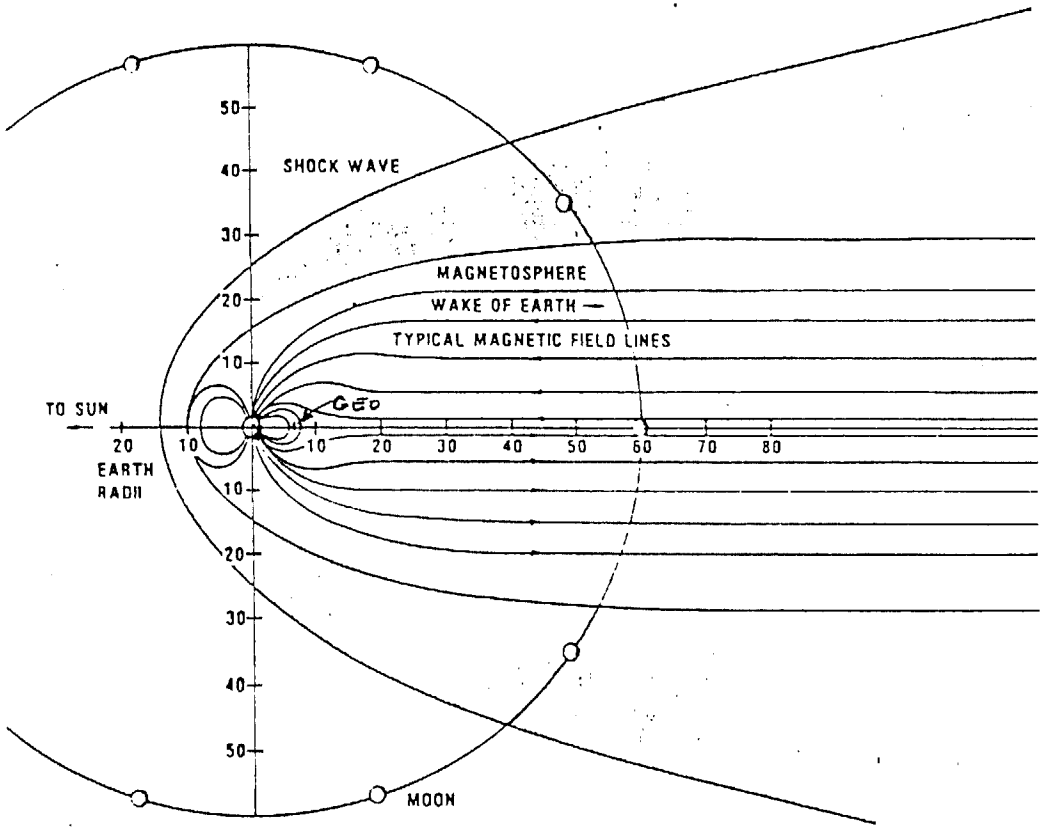

Fig. 6. Cross section of the magnetosphere showing the approximate size in terms of number of Earth radii (1 Earth radius = 6,370 km). Geostationary orbits are at 6.6 Earth radii.

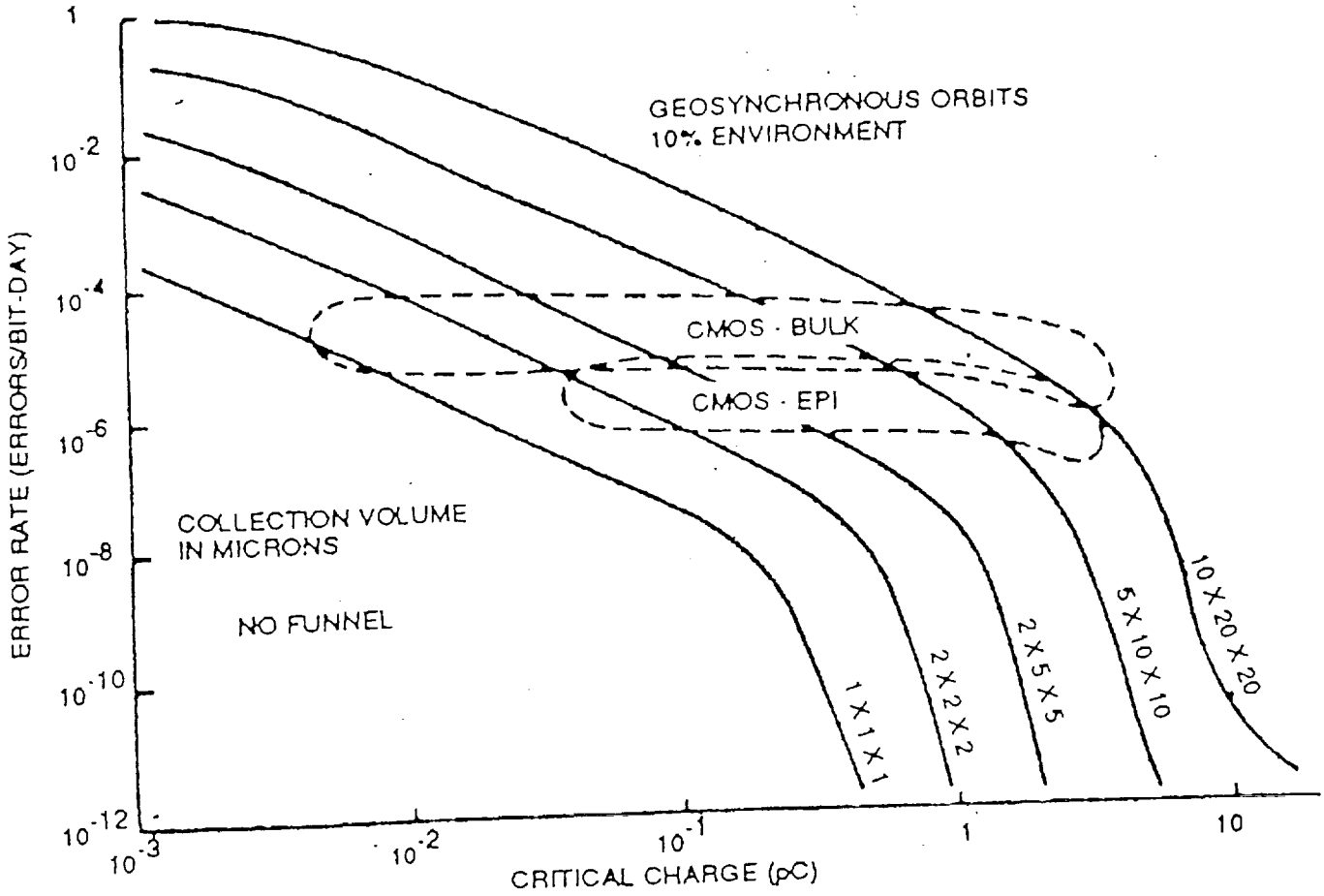

Fig. 7. Cosmic ray upset rates *(after Cunningham, 1984).*

altering on-board computer memory, evoking spurious commands. A low voltage solid-state instrumented vehicle has been flown (Scatha; spacecraft charging at high altitudes) to test various hypotheses concerning the charge-discharge situation. As described (5) p. 97 photo-emission and plasma bombardment are involved in a fashion too complicated to address here. Further, cosmic ray insult is succinctly documented per Cunningham, Circa 1984, (see Figure 7). In that there is a limitation of on-board shielding due to launch-weight constraints, great attention must be paid to orbital and mission trajectory shapes to minimize residency time in an environmentally hostile locale. An exact interpretation of all observations made thus far is yet to be made.

Efforts to deal with spacecraft-system electrification has, indeed, impacted the literature. In reviewing various references one such document[3] gives a very scholarly and detailed investigation into this matter, concluding with specific recommendations for "passive" and "active" strategies to reduce this hazard. In another well written highly detailed document[4] the entire procedure has been made into what may be described as a lengthy protocol, detailing exotic methods, such as the NASA Charging Analyzer Program (NASCAP), in which various equivalent spacecraft-system designs are analyzed, giving recommendations for optimal results in dealing with the charging hazard.

Finally, documents surfaced that deal with reactions to these hazards at the level of the microelectronic components currently in use in the circuitry of such systems. In this regard, we quote one such document[3] directly: "The methods of reducing space electrification and protecting the onboard systems against the effects of static electricity can be divided into passive and active. Passive methods are currently the principal ones used aboard geostationary satellites and other spacecraft. They include special methods of designing the spacecraft so that the units and sub-units

have good electrical contact with the metal hull of the spacecraft. Special attention is paid to the reliability of the electrical connection of the shielding jackets of the numerous electrical cables to the hull, etc. The spacecraft design should have the minimum possible number of apetures, cracks, sharp projections, to lower the likelihood of formation of greatly different electric fields.

Fiber optic communication systems within a spacecraft have an excellent prospect for enhancing the resistance of the electronic modules of a spacecraft to electromagnetic noise". ←(end of quote) Design details and suggestions, citing a specific case of satellite system malfunction (West European Satellite Marex-1) which was allegedly due to insufficient attention to the question of spacecraft charging during the design phase. In view of the above discussion, the relation between radiation hazard and deleterious spacecraft-system charging has been objectively documented.

At this point, we now move on to the next hazard for consideration; that of asteroidal and cometary meteoroids, which, in their own right, are of extreme importance in the geo-lunar realm. Because of this importance cometary and asteroidal meteoroids shall be given detailed consideration.

2.2 Meteoroid and Micrometeoroid Hazard

We now address a much less prevasive but much more severe geo-lunar hazard; that of collision with extra-terrestial particles having a wide range of masses as well as velocities. The two primary sources of these extra-terrestial entities are (a) debris left by comets in their path about the sun, and (b) debris from the asteroid belt lying in an orbital band between Mars and Jupiter (see Section 5 of Ref. 5).

Of the particles nearing the near earth-lunar environment, as best as can be documented, 90% are of cometary origin while the remaining 10% are of

astroidal origin. In assessing the overall direct collision risk[5] the opinion is given that impaction between a spacecraft-system and an object of "large size" is of such low likelihood that it can be ignored. Of those objects remaining, one can divide them into two populations, that of "shower" and that of "sporatic" meteoroids. Inasmuch as "meteor showers" vary in overall flux by a factor of the order of a hundred fold from quiescence to maximum[5], the "periods" of eighteen distinct showers have been assessed and documented[9] (see Figs. 8a and 8b).

Investigators in this subject have defined a specialized parameter, the so-called "activity" factor, which is the measure of dirunal flux change. It is defined as the ratio $F = \frac{\text{cometary flux}}{\text{sporatic flux}}$; detailed graphs of F are shown in Figs. 8a and 8b. As a consequence of the predictability of the shower flux, coupled with the dramatic changes in the "activity" factor F, F maximums can be avoided in the case of interplanetary spacecraft excursions by appropriate adjustment of launch parameters. Such adjustments are possible because the orbits of these showers are further constrained with respect to the plane of the ecliptic in a fixed direction associated with each.

This leaves the risk of sporatic (astroidal) meteoroids to be considered. In studying the literature, it was found that the treatment of meteoroids in Ref. (9) is far more stringent than in Ref. (5) Section 5. Dominant factors addressed are; classification of objects with respect to size and density, and meteoroid flux as a function of mass and number-mass distribution as a function of velocity range. The above can, for practical risk assessment purposes, be viewed as the minimum apriori information necessary for consideration of protective measures in the event of impaction of a space vehicle propulsion system. For very small particle sizes, ($<10\mu$

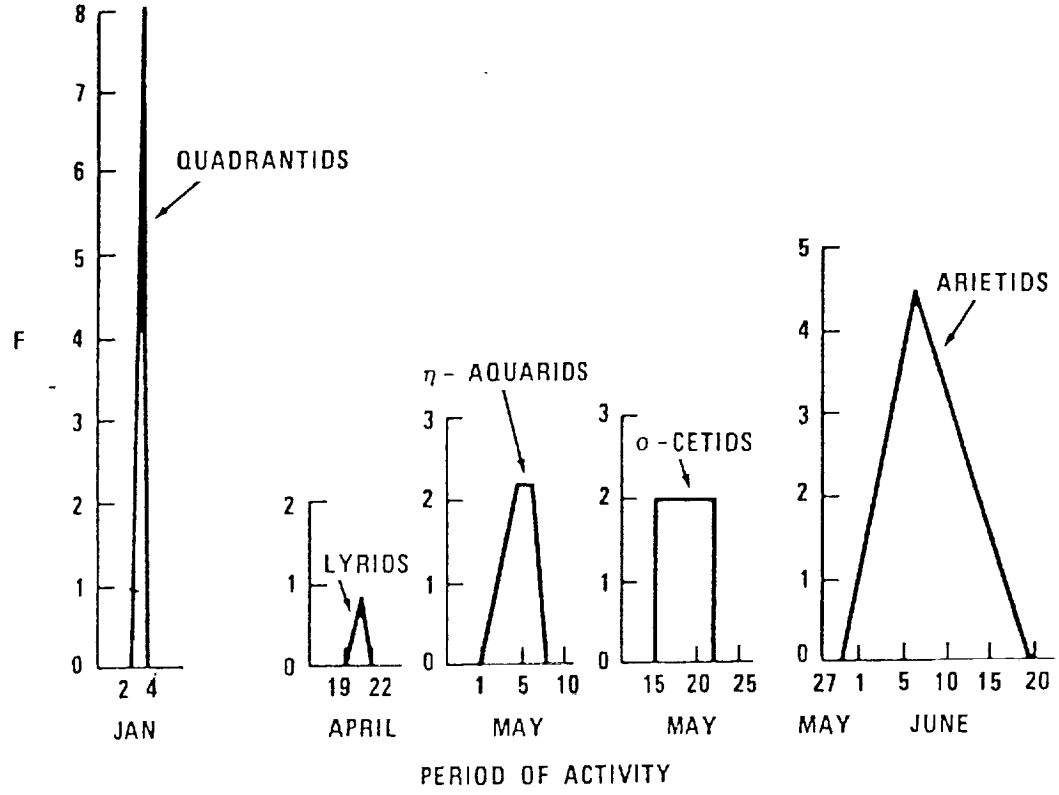

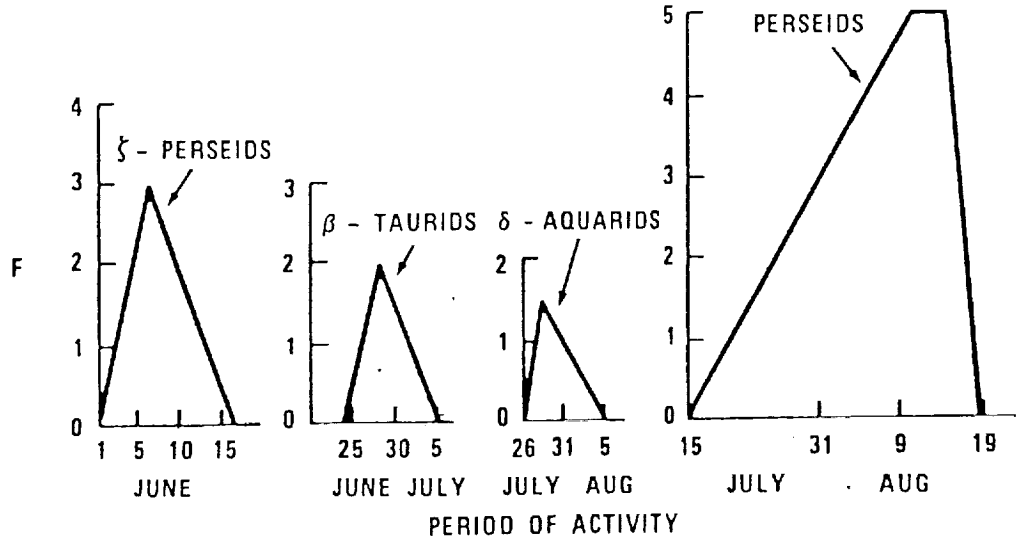

$$F = \frac{\text{CUMULATIVE FLUX OF STREAM}}{\text{AVERAGE CUMULATIVE SPORADIC FLUX}}$$

Figure 8a.–Activity ratio factor versus period of activity (January-August) for major streams based on photographic meteors with mass, $m \geq 10^{-1}$ gram.

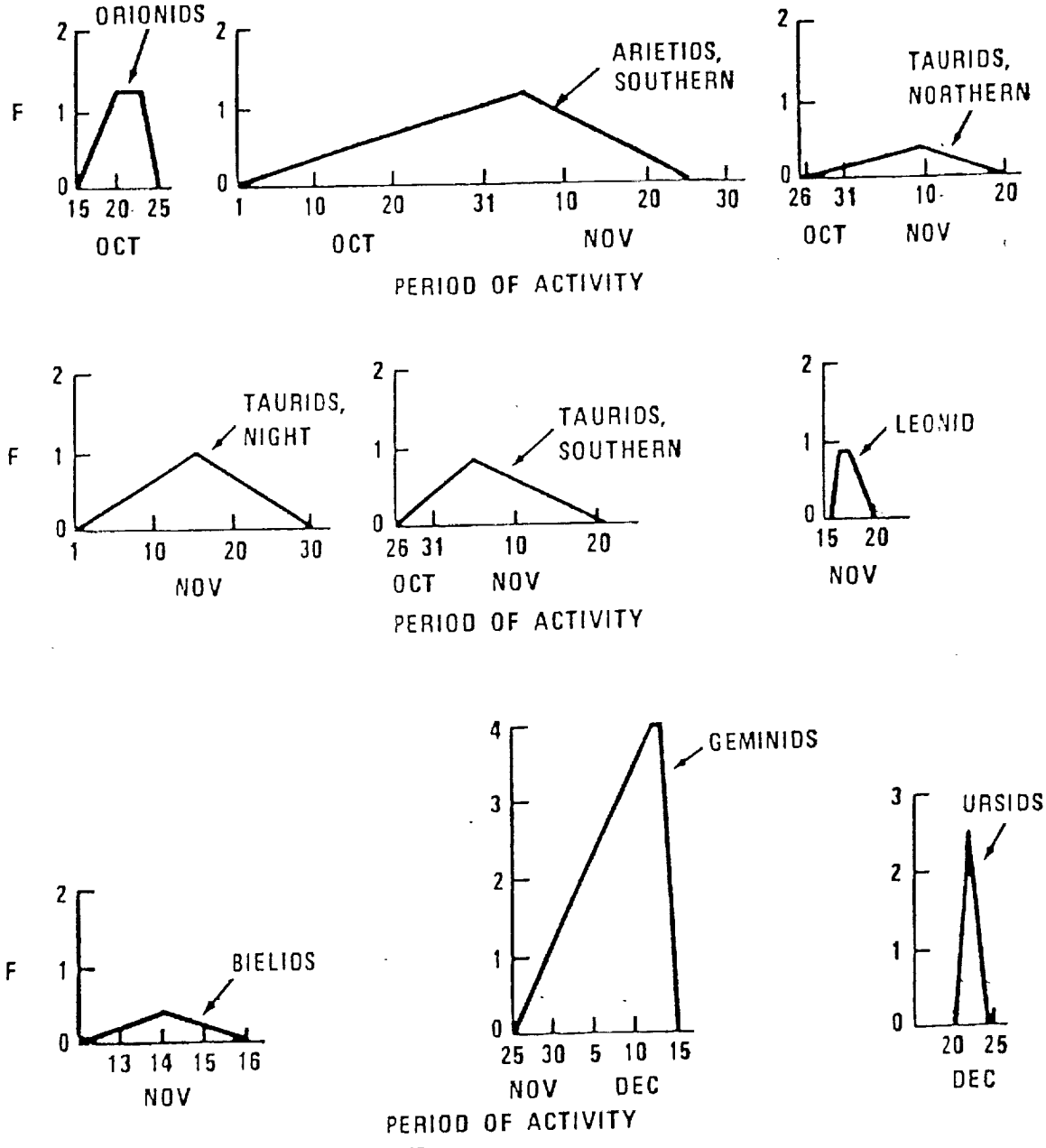

$$F = \frac{\text{CUMULATIVE FLUX OF STREAM}}{\text{AVERAGE CUMULATIVE SPORADIC FLUX}}$$

Figure 8b.–Activity ratio factor versus period of activity (September-December) for major streams based on photographic meteors with mass, $m \geq 10^{-1}$ gram.

diameter) the primary mode of damage to a spacecraft was due to surface erosion, which "proper" design and construction of the outer hull can mediate.

At the time of writing, however, little if any information existed concerning flux parameters. This leads to three aspects of the overall meteroid protection (damage management) situation: (a) the form of the flux-velocity and flux-mass size distributions, (b) detailed consideration of impact mechanisms, (c) further investigation of quantitating damage in virtue of (1) amount, (2) pattern, (3) mechanisms of damage and finally, (4) strategies for damage minimization. Detailed description of (a) is addressed in various references which were published circa 1963-1970. Of these references (6) affords the most comprehensive treatment for (a) above, in that tools of observation and acquisition of a database are clearly given; over and above this, the total meteoroid environment is divided into average, sporatic and stream meteoroids, with copious information regarding particle density, particle velocity, and attendant flux-mass emperical models. Additionally, the lunar ejecta environment is included under the "umbrella" of the mathematical models for sporatic meteoroids per-se. This gives unity to the entire mathematical description from L.E.O. to the lunar surface. For categories (b) and (c) a rather detailed treatment of these is given in reference (5) Section 5 although (7) and (8) are clearly a detailed update on this based on flight experience.

Summarizing part (a) of the meteoroid environment is best presented by examining the results of reference (6) starting with Section (3) of this document. The model summarized therein with its attendant flux-mass models and associated particle density and velocity distributions, should be used to establish the meteoroid environment for engineering application to space missions in near-earth orbit, cislunar space, lunar orbit and lunar surface. In opposition to some of the working assumptions of reference (5) Section 5

we have the following definitions of the elements of a geo-lunar meteoroid environment[6].

The meteoroid environment includes only particles of cometary origin and has a sporatic component restricted to particles whose mass m is 10^{-12} gram $\leq$ m $\leq$ 1 gram, and an additional component of stream meteoroids whose masses lie in the range 10^{-6} grams $\leq$ m $\leq$ 1 gram. (This exclude L.E.O. debris and artificial debris from L.L.O., and transfers to the lunar surface.)

2.2.1 The Average Total Meteoroid Environment

The average total meteoroid environment is the average sporatic plus a derived average stream environment, and is employed for preliminary design, and for mission intervals that cannot be specified. When a mission launch date and duration are specified later in a specific design, the probability f stream damage should then be evaluated (see sporatic & stream meteoroids below). The attendant model is given by the following expressions:

(1) Particle density is taken to be 0.5 gram/cm^3.

(2) Particle velocity is taken to be 20 km/sec with the probability distribution shown on Page 4, Fig. 1 of Ref. 2.

(3) The following emperical flux-mass model:

10^{-6} grams $\leq$ m $\leq$ 1 gram (mass range)

$$\log_{10}N_t = -14.37 - 1.213 \log_{10}m$$

10^{-12} grams $\leq$ m $\leq$ 10^{-6} gram (mass range)

$$\log_{10}N_t = -14.339 - 1.584 \log_{10}m - 0.063 (\log_{10}m)^2$$

where:

N_t = Number of particles mass m or greater per meter^2/sec

m = particle mass in grams

The above model applies to the average total meteoroid environment in the absence of perturbing influences. In the geo-lunar case, there are two phenomena that influence the actual flux encountered in the spatial domain of interest. The phenomena in question are the shielding and gravitational effects of the earth and moon. The differences in the cometary meteoroid environment near the earth and moon have been calculated, as well as the decrease of flux with distance from the earth. Consequently, the flux, particularly that of the slower moving meteoroids, that has been deduced by earth-based observational techniques and direct orbital measurements is assumed to have been enhanced by the earth's gravity. Simply stated, the earth's gravitational field increases it. Thus, the sporatic flux can be said to be gravitationally focused.

In addition to this the actual number of meteoroid impacts encountered by a spacecraft-system it is also influenced by its orbital distance above a body that provides shielding. The earth and moon can act as shields to reduce the number of sporatic meteoroids, as well as block the impacts of stream meteoroids when the orbital paths of the spacecraft-system, earth or moon, and a stream are so aligned.

To account for the earth's gravitational enhancement at a specified distance from earth center, the average sporatic or total meteoroid flux must be multiplied by an experimentally obtained defocusing factor G_e, as given in Fig. 9. The flux of stream meteoroids as affected by the gravitational influence of the earth moon system is assumed negligible because of their higher velocities.

In virtue of actual flight experience it has been determined that the number of impacts experienced by a spacecraft-system shielded by the earth or moon or as seen by a spacecraft component shielded by the spacecraft, depends on the spacecraft or component shape, and on its orientation with

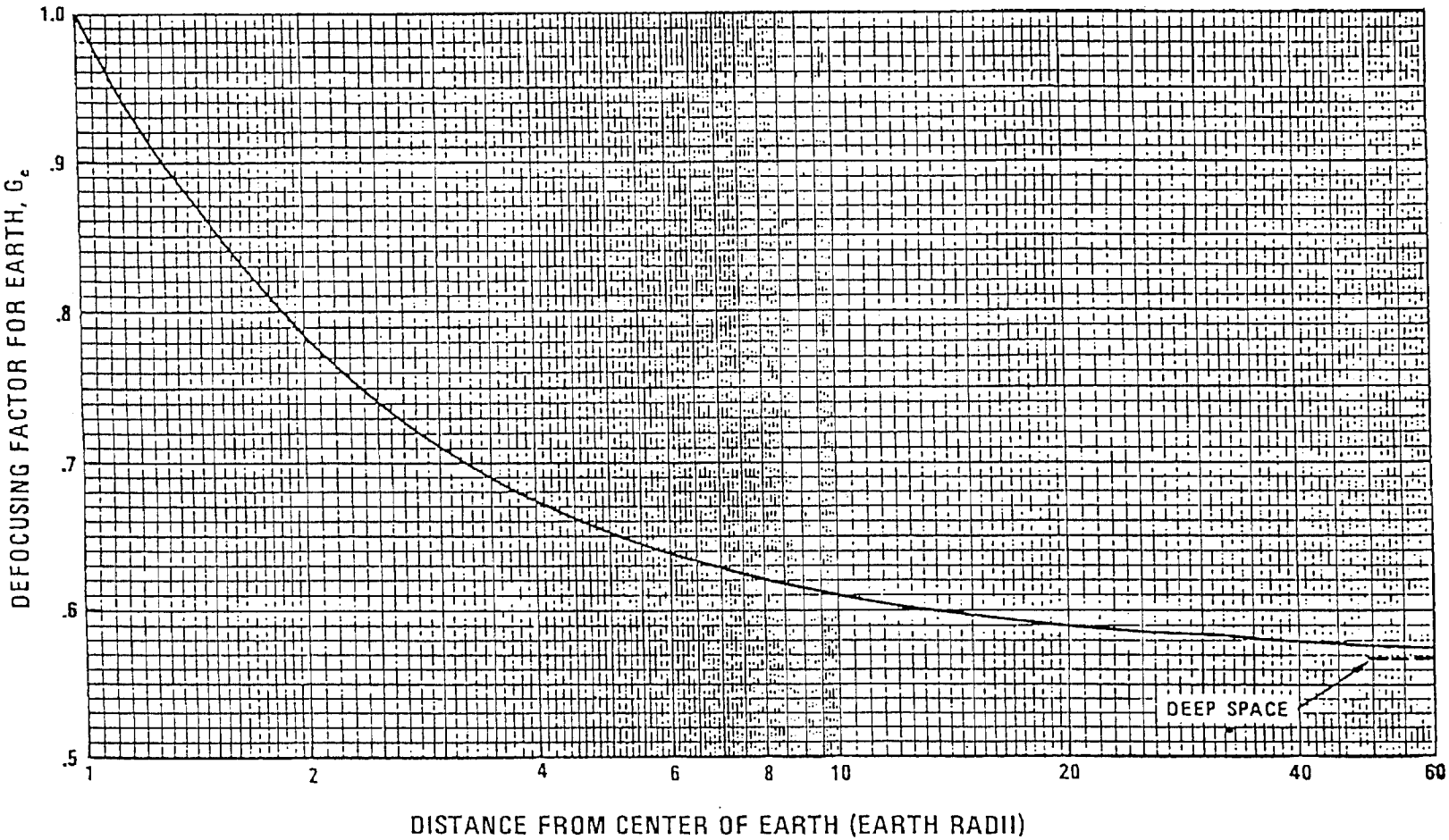

Fig. 9. –Defocusing factor due to Earth's gravity for average meteoroid velocity of 20 km/sec.

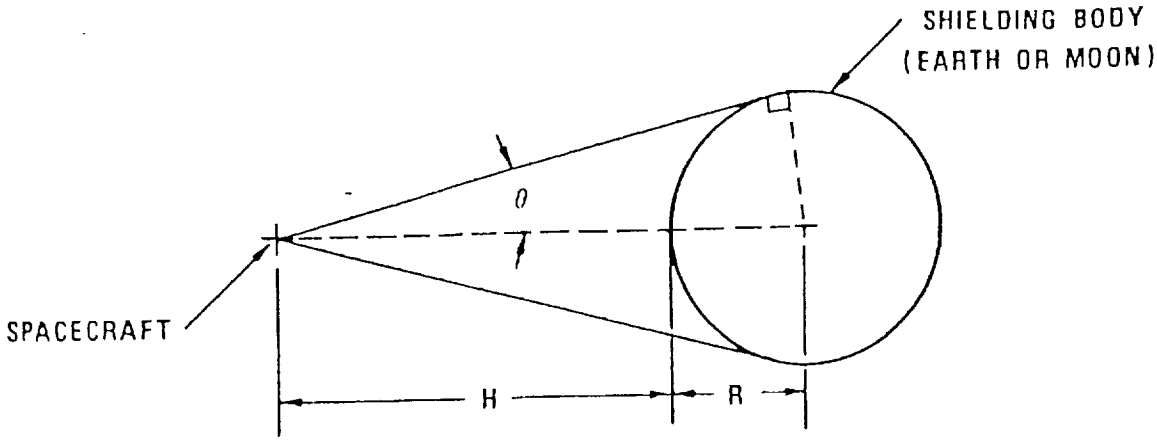

BODY SHIELDING FACTOR, ζ : (Defined as ratio of the shielded to unshielded flux)

$$\zeta = \frac{1 + \cos\theta}{2}$$

WHERE:

$$\sin\theta = \frac{R}{R + H}$$

R Radius of Shielding Body

H Altitude above Surface

Subscripts:

e Earth

m Moon

Fig. 10.—Method for determining body shielding factor for randomly oriented spacecraft.

respect to the shielding body. If the spacecraft is spherically shaped and randomly oriented, the actual number of impacts turns out to be the product of the unshielded defocused flux and the shielding, factor ζ, as specified in Fig. 10 for earth or moon.

One can think of multiplying by the factor ζ as having the effect subtracting out the flux within the solid angle subtended by the shielding body (Fig. 10).

Experience shows that, although ζ is based on a spherical spacecraft-system, the factor, ζ, will produce inconsequential differences in the actual average sporatic or total meteoroid flux impacting a spacecraft of any shape provided that it's randomly oriented. For oriented spacecraft, body shielding effects have to be considered on an individual design basis, in that shielding affects only the side toward the shielding body. In similar fashion body shielding effects applying to stream meteoroids must be determined on an individual basis.

To complete the presentation of the overall meteoroid environment in the geo-lunar domain, the remaining relevant models are now given below.

2.2.1a The Sporatic Meteoroid Environment

As in the case of the average meteoroid environment, the mass density is taken to be 0.5 grams/cm^3 for <u>all</u> sporatic particle sizes, as well as the same velocity distribution. The flux-mass model on the other hand is altered slightly, and is given as:

10^{-6} grams $\leq$ m $\leq$ 1 gram; (mass range)

$$\log_{10} N_{sp} = -14.41 - 1.22 \log_{10} m$$

10^{-12} grams $\leq$ m $\leq$ 10^{-6} gram (mass range)

$$\log_{10} N_{sp} = -14.339 - 1.524 \log_{10} m - 0.063 (\log_{10} m)^2$$

where:

N_{sp} = The number of sporatic particles in grams per meter^2/sec

m = Mass of particle in grams.

The same discussion made previously in regard to the defocusing factor G_e and shielding factor ζ apply here as well.

2.2.1b The Derived Average Stream Meteoroid Environment

Data applicable to a specific meteoroid stream environment must be employed in the design of a vehicle-system with specified launch date and mission duration. This data also provides the means of determining the probability of stream damage to vulnerable structures of a spacecraft-propulsion system that has been designed to an average total meteoroid environment. As before, particle mass densities are taken to be 0.5 gram/cm^3 for all stream particle sizes. Particle velocities are determined from each stream in Table VI. The emperical mathematical model for flux-mass for the meteoroid stream environment is given by:

10^{-6} grams $\leq m \leq 1$ gram; (mass range)

$$\log_{10} N_{st} = -14.41 - \log_{10} m - 4.0 \log_{10} \left(\frac{V_{st}}{20}\right) + \log_{10}(F)$$

where:

N_{st} - The number of stream particles of mass m or greater per meter^2/sec

m - Particle mass in grams

V_{st} - The specified geocentric velocity of each stream in km/sec from Table VI cited above.

"F" - The integrated averaged ratio of the cumulative flux of stream meteoroids to the average cumulative flux of sporatic meteoroids as calculated from Figs. 8a and 8b for the portion of the stream's duration with the mission period.

The gravitational factor, G_e, is not applied to the flux of a specific stream; further, the shielding factor ζ is not applied unless a shielding body eclipses the vehicle relative to the source stream given by Table VI. In the event of eclipse, the flux of the relevant stream is taken to be zero.

2.2.2 Lunar Ejecta Environment

To complete the modeling of the lunar meteoroid environment, we must take into account the secondary consequences of meteoroid impaction of the moon. Missions in L.E.O. or at the lunar surface will fall under the influence of the lunar ejecta environment which consists of particles of lunar material ejected from the surface of the moon by meteoroid bombardment. This can have undesirable effects on extra-vehicle activities, and other critical activities at or near lunar surface; thus, it is

TABLE VI

MAJOR METEOROID STREAMS

Name	Period of activity	Date of maximum	F_{max} (a)	Orbital elements (defined in fig.5)							Velocity
				Ω, deg.	π, deg.	ω, deg.	i, deg.	e	q, A. U.	a, A. U.	Geocentric, km/sec
Quadrantids	Jan. 2 to 4	Jan. 3	8.0	283	92	188	87	0.66	0.97	1.7	42
Lyrids	Apr. 19 to 22	Apr. 21	0.85	30.5	--	210	81	0.88	0.90	--	48
η - Aquarids	May 1 to 8	May 4 to 6	2.2	45	152	108	162	0.96	0.66	17.95	64
σ - Cetids	May 14 to 23	May 14 to 23	2.0	238	89	211	34	0.81	0.11	1.3	37
Arietids	May 29 to June 19	June 6	4.5	77	108	29	21	0.94	0.08	1.6	38
ζ - Perseids	June 1 to 16	June 6	3.0	78	--	59	4±2	0.79	0.35	1.6	29
β - Taurids	June 24 to July 5	June 28	2.0	278	182±4	246±4	8±4	0.86	0.36	2.5	31
δ - Aquarids	July 28 to Aug. 5	July 28	1.5	306	101±2	158±2	24±5	0.96	0.66	1.6	48
Perseids	July 15 to Aug. 18	Aug. 10 to 14	5.0	142	--	155	114	0.96	0.97	23	60
Orionids	Oct. 15 to 25	Oct. 20 to 23	1.2	29.3	103	67.8	163	0.62	0.54	0.32	66
Arietids, southern	Oct.1 to Nov.28	Nov. 5	1.1	27	150	122	6	0.85	0.30	1.91	28
Taurids, northern	Oct. 28 to Nov. 22	Nov. 10	0.4	221	160	308	2.5	0.86	0.31	2.16	29
Taurids, eight	Nov.1 to Nov.30	Nov.15	1.0	220	160	300	3	0.86	0.3	2.1	37
Taurids, southern	Oct. 28 to Nov. 22	Nov. 5	0.8	45	157	112	5.1	0.85	0.36	2.39	28
Leonids southern	Nov. 15 to 20	Nov. 16 to 17	0.9	234	48	178	162	0.92	0.98	12.8	72
Bielids	Nov. 12 to 16	Nov. 14	0.4	250	109	223	13	0.76	0.88	3.8	16
Geminids	Nov. 25 to Dec. 17	Dec. 12 to 13	4.0	261	--	324	24	0.90	0.14	1.4	35
Ursids	Dec. 20 to 24	Dec. 22	2.5	270	--	210	50 ±3	1.0	0.82	--	33

(a) F_{max} = Ratio of maximum cumulative flux of stream to average cumulative sporadic flux (Ref. 6)

mandatory that lunar ejecta are considered. The lunar ejecta environmental model presented here applies from lunar surface to an altitude of ≃ 30 km with velocity ranges chosen such that this mathematical model is consistent in mathematical form with those previously given. The effects of the ejecta environment is a matter of separate consideration from meteoroids due to their diverse velocity regimes. The mathematical model for this environment is as follows:

Particle Density is taken to be 2.5 grams/cm^3 for all ejecta particle sizes. For the average total ejecta flux-mass model one has on a cumulative annual basis for the following relations to be used in preliminary design:

Velocity Range:	Mass Number-Flux Relation
$0 \leq V_{ej} \leq 1.0$ km/sec ;	$N_{ejt} = -10.75 - 1.2 \log_{10} m$

N_{ejt} = Number of ejecta particles of mass m or greater (per meter^2)/sec. An average of 0.1 km/sec is to be employed with the above distribution model.

An average annual individual cumulative lunar ejecta flux-mass distribution for each of these velocity intervals for detailed study of the lunar ejecta hazard is given by:

Velocity Range:	Mass Number-Flux Relation
$0 \leq V_{ej} < 0.1$ km/sec ;	$\log_{10} N_{ej} = -10.79 - 1.2 \log_{10} m$
$0.1 \leq V_{ej} < 0.25$ km/sec ;	$\log_{10} N_{ej} = -11.88 - 1.2 \log_{10} m$
$0.25 \leq V_{ej} < 1.0$ km/sec ;	$\log_{10} N_{ej} = -13.41 - 1.2 \log_{10} m$

This formulation is of great value in view of the suggested manned moon base as a prelude to more extensive spatial exploration. It should be appreciated that the same functional forms, i.e. logarithmic, were desired as were utilized in modeling meteoroid sporatic and stream flux. To accomplish this, it was found in the interest of "goodness of fit" that the statistical fit had to be made "piecewise", breaking the velocity V_{ej} into the three ranges given.

In the above we have outlined the detailed specification of the meteoroid flux in the geo-lunar domain including near and lunar surface; we now turn our attention to analyzing the effects of this adverse space environmental component. Accordingly we now consider category (b) above, the details of impact mechanisms. Reference (5) Section 5 gives a rather detailed but dated discussion of these effects; consequently, the focus of attention shall be on Reference (7) in which categories of meteoric insult are given as follows: (1) catastrophic rupture, (2) leakage, (3) deflagration, (4) vaporific flash, (5) reduced structural strength, and finally, (6) erosion. As indicated in (7) these modes of damage to the typical spacecraft-propulsion system are dramatically demonstrated experimentally by meteoroid detection satellites, such as explorer XVI and XXIII, as well as three pegasus vehicles at the time of writing (circa 1970). Recently, the successful recovery of the LDEF by shuttle will add extensively to this data. Although the focus of evaluation of document (7) excludes mechanical or electrical components and crew injury, it's clear that damage in the context considered, indeed, has a potentially disasterous effect on them as well. In general, the response of any structure under meteoroid impact depends on five factors: (1) material composition, (2) temperature, (3) severity of stress, (4) thickness, (5) number of plates composing a structure and fabrication technique. Specification of damage is evaluated by analytical methods and other criteria in consort with physical testing. Requirements for meteoroid damage abatement are necessarily of immediate interest to those engaged in the design of ancillary systems, most notably, thermal insulation, thermal protection, space radiators, and radiation protection systems, etc. when incorporated into the overall structure. The document loc. cit., then goes on to specify "the state of the art" circa its publication. It is further stated that current knowledge in the subject (as expected) is based on numerous theoretical and experimental investigations, and points out that the two modes of approach

have led to conflicting conclusions, thus, under-scoring the inherent incompleteness of existing techniques, as well as recognition of damage categories applicable to specific structures under consideration.

Applying the above model of the meteoroid environment, a methodology of meteoroid damage assessment is required for a velocity range of 1 km/sec $\leq$ 72 km/sec relative velocity for arbitrary collision angles. The methodology must be correct in prediction for meteoroids varying from porous highly frangible objects with a density of $\simeq$ 0.5 gram/cm^3 to solid particles up to a density of $\simeq$ 8 grams/cm^3. Analytic methods give useful information for simple geometries and structures only. The more complicated require auxiliary testing and experimental techniques to be devised. The consequence of this is that velocity ranges distinguished by physical response are defined, rather than actual numerical values for speeds (see Table VII). In Section 2 of Ref. 7 experimental hardware is described in concise detail, as to projection methods and projectile types; "particle accelerators" and characteristics thereof are presented in Table VIII. One of the disadvantages of this type of equipment is emphasized: the need to greatly reduce particle size (mass) to achieve adequate experimental velocities, requiring extensive size reduction of the model or a test structure; as stated "an extremely dubious procedure". In that velocity limitations constrain the value of experimental techniques, collateral theoretical techniques are in place, particularly in the hypervelocity range. To this end, hydrodynamic theory is employed for study of hypervelocity impact of solid or porous projectiles on a "semi-infinite body" i.e., one whose lateral dimensions are large with respect to the size of impact craters produced. Although of utility, interaction of projectiles with a space craft structure often involves several types of damage, and, even the most advanced hydrodynamical models do not adequately encompass all combinations of damage. In the detailed application of the hydrodynamical

TABLE VII

SPORADIC FLUX-MASS DATA FROM PENETRATION MEASUREMENTS

SPACECRAFT	SENSOR MATERIAL	K_1	SENSOR THICKNESS t (cm)	CHARACTERISTIC MASS m (gm)	CUMULATIVE FLUX N_{sp} (m^{-2} -sec^{-1})	LOG_{10} m (gm)	$LOG_{10} N_{sp}$ (m^{-2} -sec^{-1})
PEGASUS I, II, III	ALUMINUM 2024 - T3	0.54	0.0406	5.20×10^{-7}	8.00×10^{-8}	-6.28	-7.10
			0.0203	7.25×10^{-8}	3.44×10^{-7}	-7.14	-6.46
EXPLORER XXIII	STAINLESS STEEL TYPE 302	0.32	0.0051	6.29×10^{-9}	3.33×10^{-6}	-8.20	-5.48
			0.0025	8.28×10^{-10}	5.68×10^{-6}	-9.08	-5.25
EXPLORER XVI	BERYLLIUM COPPER BERYLCO NO. 25	0.30	0.0051	7.55×10^{-9}	2.66×10^{-6}	-8.12	-5.58
			0.0025	9.95×10^{-10}	5.18×10^{-6}	-9.00	-5.29

TABLE VIII - CHARACTERISTICS OF OTHER PARTICLE ACCELERATORS

Type	Reference no	Capability	Comment no.
Electric-arc lithium plasma	6	Typical velocities 12 to 14 km/sec with particle mass from 10^{-8} to 10^{-6} g. Maximum velocity, 20 km/sec.	1, 2, 3
Electrostatic	7	30 km/sec with submicron-size iron particle. Higher velocities potentially possible.	1, 3
Exploding foil	8, 9	8 km/sec with particle mass of a few milligrams.	4, 5
Hotshot tunnel	10	30 km/sec with particle mass of approximately 6×10^{-8} g	1, 3, 4, 6
Shock tube	11	Potential velocity of approximately 9 km/sec with multiple particles 1 to 4 μ in size.	1, 3, 4, 6

Comments

1. Unsuitable for penetration tests of most actual structures because of small mass of particle.
2. Particularly suitable for penetration-mechanics research on simple targets.
3. Can launch multiple particles; has possible application for meteoroid-erosion tests.
4. Difficult to control and determine the particle parameters.
5. Possible particle breakup.
6. Possible particle ablation.

model, time dependent compressible flow equations of state are solved numerically. As of publication[7] of this study, the maximum size of the problem undertaken was limited to the two-dimensional case (an axi-symmetric projectile impacting normally to the surface of plate). For impaction at an angle, approximations must be used; 3-D mathematical representation was at time of publication, under development for direct solutions for oblique impact, which at present has been addressed in great detail (8). The above experimental and theoretical techniques serve to characterize the damage that occurs. Meteoroid impact damage circa publication of (7) was found to be best represented by the following descriptors:

(1) Partial penetration (and/or) surface damage

(2) Perforation

(3) Local deformation, spall fracture, or retached spall (back surface)

(4) Secondary fracture

(5) Catastrophic rupture

collaterally with this, several of the parameters of the overall scheme of damage are reviewed viz. semi-infinite body representation, effect of projectile density, diameter, effect of impact angle target characteristics; this followed by (p. 9 loc. cit.) a detailed discussion of thin plates; and multiplate structures.

This is in turn followed by an indepth presentation of the topic of debris and resultant damage characteristics; Figs. 11 & 12 give an excellent visual overview of results.

Subsequently, a highly informative section concerning penetration to resistance in terms of structure configurations is developed, along with a discussion of laminated plates and reinforced plastic structures. To conclude the first part of this work a concise discussion of subsystems of interest is given; namely: pressure cabins, tanks, and special purpose

surfaces. On p. 26 loc. cit. a comprehensive summary of the previous topics and their interrelationships is given.

This now leads logically to design criteria in Section 3, p. 27, loc. cit. "The structural design of the space vehicle shall ensure that damage which may result from meteoroids does not constitute an undue hazard to flightworthiness."

The document[7] then considers several aspects of the application of the criteria: meteoroid environment: meteoroid hazards are to be assessed on a basis of the mission profile and the best available model for the applicable mission environment or environments. Then, the degree of possible structural damage shall be determined by analysis and applicable experimental data. The damage assessment is to be reviewed in terms of the subsystem-probable critical failure types as given by the array of Table IX. Finally the vehicle reliability is to be expressed in terms of the required probability that meteroid damage shall not endanger the flightworthiness of the vehicle, and found compatible with the specified overall reliability of the vehicle.

Attention is now turned to the specific subsystem on board; the minimum probability that each subsystem will not fail because of meteoroid damage shall be established. Given these values, the combined minimum probability for all subsystems shall not be less than the required probability that meteoroid damage will not endanger flightworthiness of the vehicle. Finally, it's required that the type and degree of damage to structural subsystems expected to be caused by meteoroid impact shall be substantiated by appropriate physical (experimental) testing. To achieve the above, the focus of the discussion now shifts to Recommended Practices as stipulated in Section 4 of (Ref. 7).

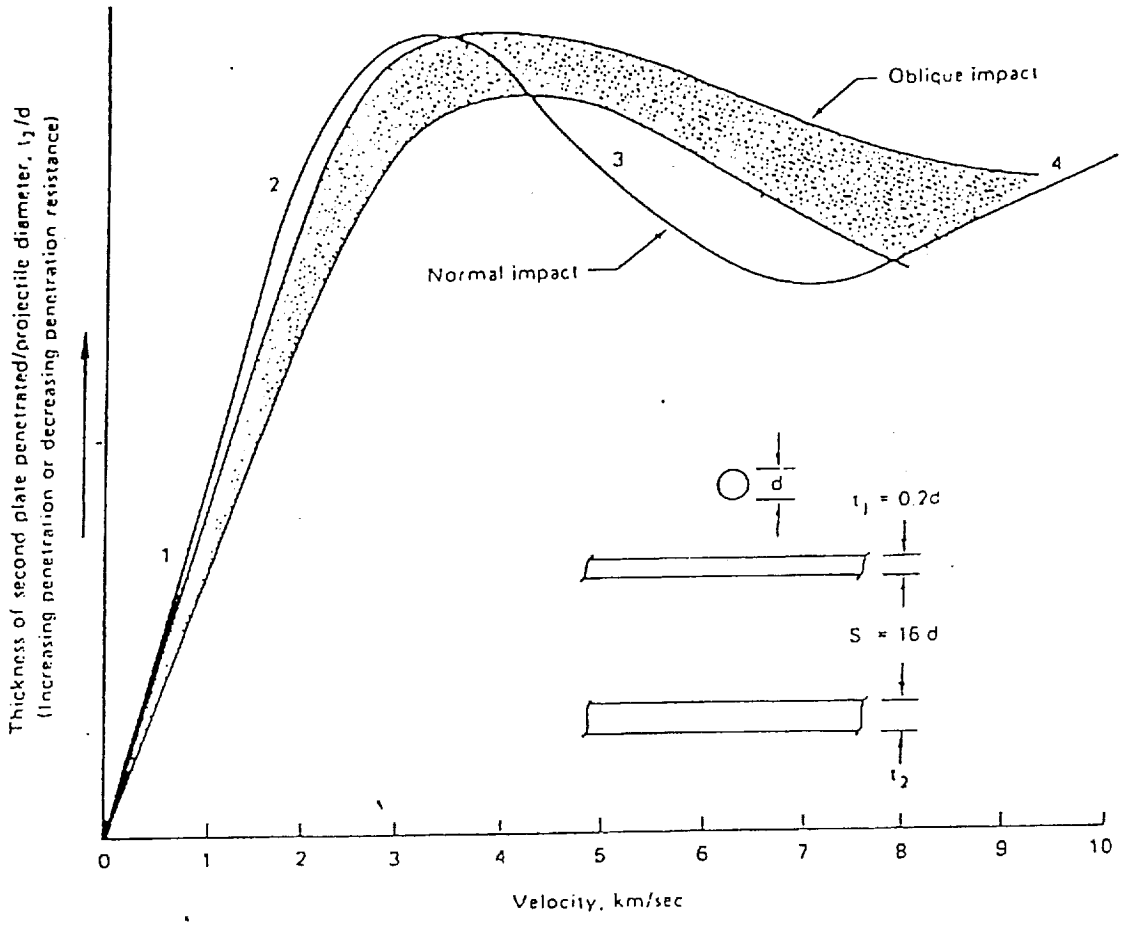

Notes:

Numbers on normal impact curve show the variation of debris with velocity

1. Intact projectile.
2. Tight cluster of relatively large fragments of projectile and shield.
3. Debris in shape of elongated bubble with surface composed of numerous small solid particles of projectile and shield.
4. Debris consisting of:
   - A. Elongated bubble composed of very small solid particles, minute drops of melted metal, and metal vapor.
   - B. A few solid fragments which are larger and slower than the balance of debris.

Figure 11 – Schematic description of how penetration resistance and debris vary with velocity (aluminum projectiles on aluminum alloy structure).

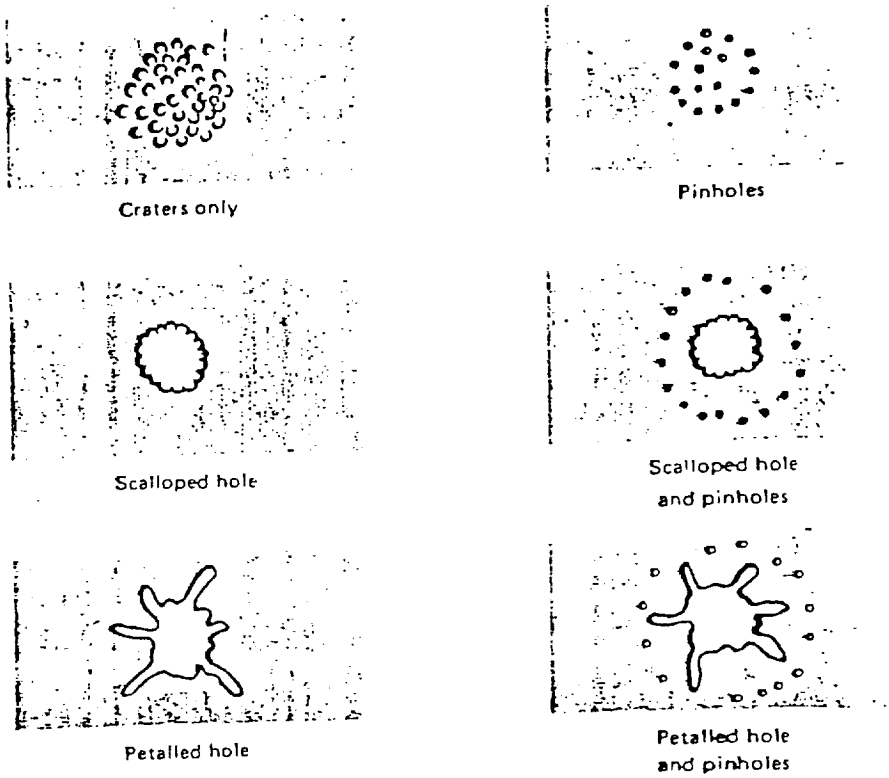

Reproduced by permission of The Boeing Co.

Figure 12 – Damage patterns on second plate of multiplate structure.

TABLE IX – PROBABLE CRITICAL TYPES OF FAILURE FOR VARIOUS SUBSYSTEMS

Probable critical types of failure	Subsystems					
	Pressure cabins	Tanks	Radiators	Windows	Special-purpose surfaces	Entry thermal protection
Catastrophic rupture	x	x		x		(To be established in terms of the specific thermal protection system.)
Secondary fractures			x			
Leakage	x	x	x			
Vaporific flash	x					
Deflagration		x				
Deformation			x			
Reduced residual strength	x	x	x	x		
Fluid contamination		x	x			
Thermal insulation damage	x	x				
Obscuration				x		
Erosion					x	

For meteoroid environment, taking into account the neighborhood of the asteroid belt, in addition to previously cited work, the probability of impact is represented by a Poisson distribution[10]:

$$P_{x \leq n} = \sum_{r=0}^{r=n} \left[\frac{e^{-NA\tau} (NA\tau)^r}{r!} \right]$$

where

$P_{x \leq n}$ = probability of impact by n meteoroids or less

N = Expected flux, (particles/m^2)/sec

A = Exposed area, m^2

τ = Exposure time, sec.

In conjunction with this probability distribution the apriori flux distribution must be modified, when appropriate, for the effects of gravitational de-focusing and shielding of the space vehicle by planetary bodies or by parts of the vehicle. Thus using the distribution given above coupled with the mathematical model of the meteoroid distribution, the probability of impaction by n or less meteoroids, and penetration depth, is in principle, a calculable quantity, for which the working equation is:

$$P_\infty = K_\infty m^{0.352} \rho_m^{1/6} V^{2/3}$$

where

P_∞ = penetration depth cm

K_∞ = an emperical constant

m = mass of meteoroid in grams

ρ_m = density of meteoroid grams/cm^3

V = impact velocity km/sec

To complete the assessment the following topics are considered: (1) methodology for a semi-infinite body, (2) methodology for thin plates

(structures), (3) methodology for subsystems, including (a) pressure cabins, (b) tanks, (c) radiators, (d) thermal protection systems, (e) windows (prts), and (f) special purpose surfaces. Having given due attention to these items, the document[7] addresses overall vehicle reliability and subsystem reliability; from the vantage point of theoretical investigation and actual testing, specifying the hardware to be used in the latter. For a current treatment of actual cases of impaction given in example form, see reference 11. All the above criteria and methods of the previous discussion have been greatly enhanced by a very recent work[8]. R. Mog et. al of Science Applications International, Huntsville, Alabama have developed a Stochastic optimal model applicable to the meteoroid impact problem. This work incorporates a space debris environment model into an overall optimization methodology utilizing engineering models developed to predict protective structural design requirements for hypervelocity impaction.

The results of this extensive study[8] indicate that careful consideration of the space platform structural configuration and materials can partially offset the design consequences of dramatic increases in the debris environment of earth and lunar orbital space. Additionally, the use of appropriate non-linear optimization techniques coupled with hypervelocity impact models can reveal significant design trade-off insights through implementation of parametric analysis.

We now consider the next hazard which is peculiar to low earth orbit, monatomic or nascent oxygen. This hazard is such that reduction thereof, is possible, and can be fabricated into the propulsion-vehicle system.

2.3 Monatomic Oxygen Hazard

This hazard applies specifically to the environment of low earth orbit (L.E.O.); it's been found that Monatomic oxygen is highly reactive in that

oxidation-reduction reactions take place with the outer hull of a space propulsion-structure system platform which erode and can (particularly on long missions) invade the propulsion system as well as other vital structures within the hull of such a device. No general review article giving a detailed exposition of this phenomenon has surfaced in the references under review at this writing. In any event, this particular aspect of the various investigated space hazards has been more fragmentary. Various abstracts addressing this source of space system degradation have been reviewed, and these documents tend to describe highly intensive efforts of studies, evaluations, and interdiction of this particular insult. None of the documents reviewed thus far give a cohesive overview of all the basic physical processes involved, but do pursue, from an experimental point of view, the scope of the situation in a pragmatic fashion. Inasmuch as this source of degradation arises in low earth orbit due to photo-dissociation at the edge of the earth's atmosphere, and many of the relevant principles of physical chemistry and material science are known, the efforts reported on, thus far reviewed, can be thought of in terms of a design goal, along with strategies to achieve the desired design goal.

The fundamental design goal is the development and synthesis of new materials that resist the corrosive effects of nacent oxygen in consort with other hazards present. Thus, through carefully planned "scout" missions, of which the LDEF is a good example, one can accumulate the experimental data required to utilize existing materials available for hull fabrication as well as develop new ones. There is in effect, an interactive data accumulation and material "development loop" that will converge on the best engineering trade-off for the desired design goal.

In viewing the documents reviewed on the above context, the following categories of active investigation reveal themselves:

A) Fabrication of land based mono-oxygen sources.

B) Fabrication of land based simulated L.E.O. and possibly other environments.

C) Investigation of various deleterious reaction mechanisms that can be clearly identified for purpose of selecting suitable resistant materials already in existence.

D) Utilize the data obtained in C) and from it deduce reaction cross-sections (in analogy to radiation transport work) for the synthesis of new more suitable materials than existing ones.

E) Design, development and calibration of flight hardware so that L.E.O. and other experimental mission results can be placed on a common baseline with those obtained in a land-based simulated environment.

Proper pursuit of these investigational categories will, indeed, result in the best possible structural design-configuration as well as material composition for the platform-propulsion system, dedicated to a long mission of choice.

Presently, forty-to-fifty abstracts have been reviewed on a basis of immediate relevance and technical merit, but it would be verbose to list all of these, except for a few compelling examples that shall be cited here[9]. The thrust of the initial document[10] considered is the development of an atomic oxygen facility constructed for the study of material degradation. The overall purpose is to establish techniques for the fabricating and configuring various material species for long-term use in L.E.O.; (twenty-to-thirty years). This effort appears very broad in scope, and, in fact essentially embraces the categories just given. In contrast to the broad approach of the previously mentioned example, the next document[11] goes into an extremely detailed description of a technology for producing a beam of mono-oxygen in consort with various types of samples fabricated with materials that show promise for use in propulsion-structure systems in

L.E.O.; note that the detail gone into cannot be pursued here. Suffice it to say 5-15 km/sec mono-oxygen beams operating in simulated L.E.O. environment are a absolutely essential component in synthesizing the material-structural components of a long-term mission oriented propulsion-platform system.

Continuing the discussion, paper[12] illustrates a companion effort to that described previously. The difference lies in the fact that an ion exchange column device is exploited. At its writing, this facility was under construction at the Lewis Research Facility. Details of the construction of the $[0]^*$ "gun" are given, and provision for simultaneous UV beam & [0] irradiation is made for material samples to be tested.

Our final exemplary reference[13] is typical of the others discussed above; a novel design and construction technique provides [0] beam production as well as collateral generation of a high temperature plasma (20,000 K°). The method of [0] beam generation is that of a pulsed molecular beam produced by a supersonic expansion nozzle, under the influence of an 18J pulsed CO_2 TEA laser, capable of 10^9 W/cm^2 intensities. This "ramming" effect produces an [0] beam whose velocity spectrum ranges from 5 to 13 km/sec, which, to be sure, is ideal for simulating L.E.O. relative velocities which are of the order of 8km/sec. Extremely important preliminary results from this facility indicate that most hydrocarbons and active metals are highly reactive, however, materials containing silicones, flourides, oxides and noble metals are moderately inert in the simulated [0] environment. Further tests were carried out on the aerospace polymer Kapton^R and measurements indicated that approximately one in ten [0] atoms interactions lead to mass loss due to chemical reactions initiated. At the writing of reference[10] the researches reported provoked the development of "hardening technologies" to subvert [0] interaction effects.

The above anecdotal accounts illustrate the tone of the abstracts reviewed; one can readily see that systematic study of the [0] space hazard can be examined in the context of the criteria previously described.

There now remains, for some discussion, the hazard of thermal gradients and shock. This hazard comes about due to light-to-shadow, or shadow-to-light, traversals of the propulsion platform-system with respect to the sun as a consequence of eclipse with the earth or moon. In addition, due to the attitude of an irregularly shaped system geometry the above can result from "self-shadowing."

2.4 Thermal Gradient and Shock

It must be realized that this hazard has multiple effects; it is a direct catalyst for (1) space-craft charging (G.E.O.) (2) enhancement of corrosive effects of monatomic oxygen in L.E.O. and (3) detrimental mechanical stressing of the exterior structure, particularly to solar panels of alar design.

In direct connection with effect (3) the question arises as to whether such mechanically induced stress could compromise either nozzle, gimbal or combustion chamber geometry. In this study, no document surfaced that would address this issue.

However, in direct reference with this hazard a recent paper[14] gives an excellent review of thermal shock disturbance analyses in relation to the TOPEX satellite. This document gives in depth analysis and discussion of the impulsive torque initiated on the large single wing-solar array when exiting earth shadow, and a "companion" impulsive torque initiated by rapid cooling of the array on entry into earth's shadow.

Sunrise-sunset torque disturbance as indicated in this document[14] has been clearly observed on orbit of the Lanstat-4 mission. It turns out to be

a dominant source of attitude perturbation during attitude determination and control subsystem normal mission mode science data collection operations. It is shown that the sunrise/sunset disturbance is primarily roll/yaw perturbation with minimal pitch axis interaction.

The document[14] goes on to describe detailed modeling, analysis and simulation of the so-called sunrise/sunset thermal shock disturbance torque. Detailed review is given to the thermo-mechanical modelling and dynamic analysis performed to characterize the TOPEX sunrise/sunset disturbance. The paper[14] concludes with detailed discussion of the non-linear three-axis time domain simulation results and summarizes the predicted on-orbit performance of the normal mission mode attitude control system in the face of the sunrise-sunset disturbance. The document[14] goes on further to indicate that this disturbance results in temporary attitude perturbations that exceed the normal mission mode requirements; but goes on to state that these perturbations are well below maximum allowable pointing error which would cause the TOPEX radar altimeter to break lock.

3.0 SPACE HAZARD INTERACTIONS

At this point in time, very definite patterns are starting to emerge. The hazards thus far investigated for the earth-moon environment indicate that there are three distinct hazard characteristics: (a) Prevasive - that's the best way to describe that which falls into the broad category of radiation. (b) Incident specific - this applies to thermo mechanical shock and meteoroid hazard with exception of that portion of meteoroid flux that is defined as dust. (c) Chemically corrosive - this term would best apply to that of monatomic oxygen in low earth orbit. It is certainly recognized that long-term degradation in the specified spatial region will be in fact a superposition of these three classes of hazards. It is quite clear however,

that probabilistic radiation models can be of great assistance in selection of viable mission trajectories as well as appropriate launch times within constraints dictated by orbital mechanics. This is also true for the meteoroid hazard as well. Thus in relation to these two types of hazards, a scheme of "risk indices" which "rate" proposed mission profiles could be developed to determine the best overall specific mission configuration in relation to these two classes of while an active rather than passive strategy must deal with the other risk. Another significant aspect of the hazards of radiation, meteoroid dust and atomic oxygen lies in that in fact that they clearly act in concert rather than in isolation. It is not clear from literature thus far, to what degree synergism applies, but it would be very surprising if one would discover that the hazards behaved in conformity with a "linear superposition" model. In dealing with the effects of these hazards from the point of view of their interactions as opposed to separate effects, development of the propulsion-platform system in virtue of appropriate definitions and attendant mathematical models when merged with earth-based simulation and real-flight experimental results can form an interactive loop as is exemplified in a recent investigation[8].

4.0 SUMMARY

In the foregoing the attempt has been made to highlight various space hazards that exist in the geo-lunar environments, and give specific examples of deleterious effects than can be visited upon a long term mission-oriented spacecraft system in low earth orbit, geostationary orbit, the intervening space to low lunar orbit and finally the lunar surface.

The hazards were further categorized as prevasive (radiation), incident specific (meteoroids and thermal shock), and chemically corrosive (monatomic oxygen). It appears that for the most part; that the common preventive

denominator for all this, both when these hazards come into play interactively (low earth orbit) and when there is less tendency for such overall interaction, is the development of new materials which is the number one priority. Secondary to this, is the appropriate fabrication of the exterior hull in such fashion that incident specified hazards can be minimized in a passive fashion. It can be seen that the prevasive hazard in its many forms must also be dealt with in a passive fashion by exploring appropriate on board circuit technology with ancilary monitoring systems.

Insofar as interdicting the propulsion system itself, it would seem that given an adequate hull, its structure should be protected, and, in the same fashion its function should be assured, given that appropriate criteria are followed actively and passively in regard to external geometry and internal circuitry and controls.

What seems not be be included in this are the effects of thermal shock on the exterior nozzle structure, the directional gimbals and internal combustion chamber geometry.

Concluding, it is now recommended that representative work[8] be applied to proposed propulsion systems and sub-systems thereof to take full advantage of newly developed materials for every engineering design trade-off possible.

Subsequent investigations shall indeed require much greater depth; in addition to the study of all possible design trade-offs the effort must be made, from the point of view of flight risk minimization, to develop mathematical models that will address the risks in conjunction with each other, such that the relative risk of two or more proposed missions can be expressed hopefully in one real number, a "risk index" "or figure of merit" for example. Furthermore, such mathematical models should be capable of rating the risk incurred by various subsystems of a vehicle and propulsion

system for a planned mission, in such a fashion that overall design parameters can be conveniently adjusted.

5.0 REFERENCES

(1) Venus and Mars Nominal Natural Environment for Advanced Manned Planetary Mission Programs, second edition, Dalas E. Evans, David E. Pitts and Gary L. Frans, Manned Spacecraft Center, Houston, Texas (1967).

(2) "Introduction to the Space Environment", T.F. Tascione, Orbit-Foundation Series.

(3) The Electrification of Spacecraft, A.I. Akishin and L.S. Novikov, NASA TM-77653.

(4) Design Guidelines for Addressing and Controlling Spacecraft Charging Effects, C.K. Purvis, H.B. Garrett, A.C. Whitney, and N.J. Stephens, NASA Technical Paper 2361.

(5) The Space Environment, General Editor N.H. Langton, American Elsevier Publishing, Inc.

(6) Meteoroid Environment Model - 1969 Near Earth to Lunar Surface: NASA SP-8013, B.G. Cour-Palais, F.L. Whipple, Ad Hoc Committee Chairman

(7) "Meteoroid Damage Assessment", NASA SP-8042, Task Manager T.L. Colman, Author V.C. Frost.

(8) Spacecraft Structures Design Optimization, R. Mog, Science Applications Int'l, Huntsville, Alabama, AIAA 90-0087, January 8, 1990.

(9) Proceedings of the NASA Workshop on Atomic Oxygen Effects, November 10-11, 1986, D.E. Brinza, Editor, JPL Publication 87-14.

(10) "High Intensity 5 ev Atomic Oxygen Source and Low Earth Orbit Simulation Facility" N87-26186 J.B. Cross, L.H. Spangler, M.A. Hoffbauer, and F.A. Archuleta, Los Alamos National Laboratory, in collaboration with L. Leger and J. Visentine, Lynon B. Johnson Space Center, JPL 87-14; N87-26186.

(11) "A Sputtering Derived Atomic Oxygen Source for Studying Fast Atom Reactions", R.A. Ferrieri, Y.Y. Chu and A.F. Wolf, Bookhaven National Laboratory, JPL 87-14; N87-26187.

(12) "Neutral Atomic Oxygen Beam Produced by Ion Exchange for Low Earth Orbital Simulation", B. Banks and S. Rutledge, NASA Lewis Research Center, JPL 87-14; N87-26188.

(13) "Pulsed Source of Energetic Atomic Oxygen", G.E. Caledona and R.H. Krech, Research Park, Andover, MA, JPL 87-14; N87-26189.

(14) Sunrise/Sunset Thermal Shock Disturbance Analysis and Simulation for the TOPEX Satellite, C. Dennehy, D. Zimbelman and R. Welch, Fairchild Space Co., Germantown, MD., AIAA 90-0470, January 8, 1990.